

Submitted to  
Physical Review

UCRL-20441 Rev. 1

STUDIES OF MENDELEVIUM ISOTOPES WITH MASS  
NUMBERS 248 THROUGH 252

Pirkko Eskola

May 1972

RECEIVED  
LAWRENCE  
RADIATION LABORATORY

MAY 8 1972

LIBRARY AND  
DOCUMENTS SECTION

AEC Contract No. W-7405-eng-48

TWO-WEEK LOAN COPY

*This is a Library Circulating Copy  
which may be borrowed for two weeks.  
For a personal retention copy, call  
Tech. Info. Division, Ext. 5545*



UCRL-20441 Rev.

34

## **DISCLAIMER**

This document was prepared as an account of work sponsored by the United States Government. While this document is believed to contain correct information, neither the United States Government nor any agency thereof, nor the Regents of the University of California, nor any of their employees, makes any warranty, express or implied, or assumes any legal responsibility for the accuracy, completeness, or usefulness of any information, apparatus, product, or process disclosed, or represents that its use would not infringe privately owned rights. Reference herein to any specific commercial product, process, or service by its trade name, trademark, manufacturer, or otherwise, does not necessarily constitute or imply its endorsement, recommendation, or favoring by the United States Government or any agency thereof, or the Regents of the University of California. The views and opinions of authors expressed herein do not necessarily state or reflect those of the United States Government or any agency thereof or the Regents of the University of California.

-iii-

STUDIES OF MENDELEVium ISOTOPES WITH  
MASS NUMBERS 248 THROUGH 252\*

Pirkko Eskola

Lawrence Berkeley Laboratory  
University of California  
Berkeley, California 94720

May 1972

## ABSTRACT

Five isotopes of mendelevium, with mass numbers 248 through 252, were studied by means of  $\alpha$ -particle spectroscopy. The isotopes were produced by bombarding  $^{241}\text{Am}$  and  $^{243}\text{Am}$  targets with  $^{12}\text{C}$  and  $^{13}\text{C}$  ions accelerated by the Berkeley HILAC. The half-lives of the nuclides and the energies of the main  $\alpha$ -particle groups were observed to be:

$^{248}\text{Md}$	$7\pm 3$ sec	$8.32\pm 0.02$ MeV
$^{249}\text{Md}$	$24\pm 4$ sec	$8.03\pm 0.02$ MeV
$^{250}\text{Md}$	$52\pm 6$ sec	$7.75\pm 0.02$ MeV
$^{251}\text{Md}$	$4.0\pm 0.5$ min	$7.55\pm 0.02$ MeV
$^{252}\text{Md}$	$2.3\pm 0.8$ min	no $\alpha$ decay

The  $\alpha$ -particle energies of  $^{245}\text{Es}$ ,  $^{246}\text{Es}$ , and  $^{247}\text{Es}$ , produced mainly by  $(\text{HI}, \alpha \text{xn})$  reactions, were measured to be  $7.73\pm 0.02$ ,  $7.36\pm 0.03$ , and  $7.31\pm 0.03$  MeV, respectively, and the half-life of  $^{247}\text{Es}$  was found to be  $4.7\pm 0.3$  min. Excitation curves for producing the Md isotopes and some other activities are presented. Estimates for the EC branching of the Md isotopes are given.  $\alpha$ -decay hindrance factors were calculated using the spin-independent equations of Preston. The  $\alpha$ -decay energy systematics of the mendelevium isotopes is discussed.

## I. INTRODUCTION

The only study of light mendelevium isotopes with  $A < 254$ , before the present work, was done by Donets et. al.<sup>1</sup> in 1965. By bombarding a  $^{238}\text{U}$  target with  $^{19}\text{F}$  ions they were able to produce and identify  $^{252}\text{Md}$ , which decayed by electron capture with a half-life of about 8 min. They also established the excitation function for the reaction  $^{238}\text{U}(^{19}\text{F}, 7n)^{250}\text{Md}$  by observing the  $\alpha$  decay of  $^{250}\text{Fm}$ , which was assumed to be formed mainly from  $^{250}\text{Md}$  by electron capture. They did not report any decay characteristics for  $^{250}\text{Md}$ .

In the present work, five isotopes of mendelevium, with masses 248 through 252, were observed and studied by means of  $\alpha$ -particle spectroscopy. The mass assignments of the isotopes were based on excitation-function measurements, on cross-bombardment techniques and on studies of genetic links to previously known isotopes of Fm and Es.

More precise values for the decay characteristics of  $^{245}\text{Es}$ ,  $^{246}\text{Es}$ , and  $^{247}\text{Es}$  were also obtained as a by-product of the study of Md isotopes.

## II. EXPERIMENTAL

A 75- $\mu\text{g}$   $^{241}\text{Am}$  and a 44- $\mu\text{g}$   $^{243}\text{Am}$  target were used in most of the bombardments. Both targets were prepared by a molecular plating method and deposited on a 2.5-mg/cm<sup>2</sup> Be foil in an area of 0.18 cm<sup>2</sup>. Either  $^{12}\text{C}$  or  $^{13}\text{C}$  beams accelerated by the Berkeley heavy ion linear accelerator were used in most of the experiments. Beams of 3-4  $\mu\text{A}$ , measured as fully stripped ions, were typically passed through the targets. The energy of the 10.4 MeV/nucleon particles was adjusted by a stack of Be metal-foil degraders and measured by a solid-state detector intercepting particles scattered from the target at an angle of 30°.

The reaction recoils from the target were stopped in helium gas in a

small chamber next to the target. The rapidly flowing gas then carried the recoils through a small orifice into a rough vacuum to be collected on a vertically mounted wheel. The wheel was periodically rotated to place the collected transmutation products next to a series of peripherally mounted Si-Au surface-barrier detectors in order to measure their  $\alpha$ -particle spectra. There were seven detector stations arranged equidistantly at  $45^\circ$  intervals around the wheel. At each detector station there were four detectors: two movable (parent) detectors which alternately faced the wheel, and two stationary (daughter) detectors to alternately face the mother detectors when they were shuttled off the wheel. By this arrangement genetically related  $\alpha$  activities could be separated from one another and detected at high efficiency. A schematic representation of the arrangement of the 28 detectors around the vertical wheel and in each individual station is shown in the recent publication on lawrencium isotopes by K. Eskola et. al.<sup>2</sup>

$\alpha$ -decay events recorded by the detectors were amplified by modular units developed in our laboratory, processed by a PDP-9 computer and stored on IBM tape. The 512-channel  $\alpha$ -particle spectra covered the range from 6 to 12 MeV. Spontaneous-fission discriminators were set to detect pulses greater than 30 MeV in each detector. Both the wheel-stepping and the shuttle period were independently divided into four time subgroups of equal length. Besides the pulse height and the event time, a detector identification signal, as well as signals indicating the prevailing shuttle condition and pertinent time subgroup, were stored by the computer. Data processing, such as spectrum fitting, normalizing the gain on the detectors, and sorting of the data was done off line by either the PDP-9 or CDC-6600 computers.

### III. RESULTS

#### 1. $^{250}\text{Md}$ , $^{251}\text{Md}$ , and $^{252}\text{Md}$

In bombardments of the  $^{243}\text{Am}$  target with  $^{13}\text{C}$  and  $^{12}\text{C}$  ions two new  $\alpha$  activities were observed: a 7.75-MeV, 52-sec activity which was assigned to  $^{250}\text{Md}$  and a 7.55-MeV, 4.0-min activity assigned to  $^{251}\text{Md}$ . The  $\alpha$ -particle spectra displayed in Fig. 1 resulted from a bombardment of  $^{243}\text{Am}$  target with 88-MeV  $^{13}\text{C}$  ions and were recorded by the movable detectors when facing the wheel. The SAMPO computer program<sup>3</sup> was used to determine the energies and relative intensities of the  $\alpha$ -particle groups. The 7.136-MeV peak of  $^{214}\text{Ra}$  and the 7.439-MeV peak of  $^{250}\text{Fm}$  were used for both shape and energy calibration.

$^{250}\text{Md}$  has a complex  $\alpha$ -particle spectrum with a prominent group at 7.75 MeV ( $\sim 70\%$ ) and a smaller group at 7.82 MeV ( $\sim 30\%$ ). The 7.55-MeV group belongs to  $^{251}\text{Md}$ .  $^{250}\text{Fm}$  is present in the spectra because the odd-odd  $^{250}\text{Md}$  mainly undergoes electron capture (EC) and  $^{250}\text{Fm}$  recoils accumulate on the wheel and on the detectors facing the wheel. The cross section for direct formation of  $^{250}\text{Fm}$  is of the order of 10% or less of the cross section for the  $^{243}\text{Am}(^{13}\text{C}, 6n)$   $^{250}\text{Md}$  reaction. Similarly, the appearance of  $^{252}\text{Fm}$  in the spectra is mainly due to electron capture in  $^{252}\text{Md}$ . The other activities (Cm, Cf) present were accumulated on the wheel and on the detectors during earlier unrelated bombardments or were induced by a lead impurity in the target (Po, Rn, Ra). The 6.63-MeV peak is mainly due to  $^{253}\text{Es}$  contamination in the measuring system.

The spectra recorded by the same detectors while not facing the wheel, combined with spectra from the stationary detectors facing them, are shown in Fig. 2. The spectrum recorded by the seventh station was omitted because of difficulties in lining up the spectra from different detectors. The 6.757-MeV peak of  $^{246}\text{Cf}$  and the 7.439-MeV peak of  $^{250}\text{Fm}$  were used for shape and energy calibration.

In these "daughter" spectra the  $^{250}\text{Fm}$  peak appears to decay with the same 50-sec half-life as the 7.75-MeV peak in the "parent" spectra (Fig. 1) confirming the assignment of the 7.75-MeV activity to  $^{250}\text{Md}$ . The  $\alpha$ -decay daughter of  $^{250}\text{Md}$ ,  $^{246}\text{Es}$ , is not seen in the spectra because of the small  $\alpha$  branching of both  $^{250}\text{Md}$  and  $^{246}\text{Es}$ . For the same reason neither the electron-capture nor the  $\alpha$ -decay daughter of  $^{251}\text{Md}$  appears as a distinct peak in the spectra: the  $\alpha$  branching of  $^{251}\text{Fm}$  is about 1%<sup>4</sup> and that of  $^{247}\text{Es}$  about 7%.<sup>5</sup> The 7.04-MeV  $^{252}\text{Fm}$  peak is due to electron capture of  $^{252}\text{Md}$ . Because of the long half-life of  $^{252}\text{Fm}$  most of the counts in 7.04-MeV peak originate from  $^{252}\text{Md}$  produced in previous bombardments with  $^{13}\text{C}$  ions. The decay curve of the  $^{252}\text{Fm}$  in daughter spectra combined from four bombardments with 72-88 MeV  $^{13}\text{C}$  ions is plotted in Fig. 3. A value of  $140 \pm 50$  sec is derived for the half-life of  $^{252}\text{Md}$  by a least-squares analysis. This is considerably shorter than the 8-min value reported by Donets et. al.<sup>1</sup>

Further evidence for the suggested mass assignments of Md isotopes was furnished by excitation function studies. Fig. 4a shows the excitation curves derived from parent spectra and Fig. 4b those from daughter spectra produced in bombardments of  $^{243}\text{Am}$  with  $^{13}\text{C}$  ions. The excitation curves in Fig. 4b have been corrected with geometry and time factors to make them comparable with the curves in Fig. 4a. The excitation function for the 7.55-MeV activity reaches its maximum at about 78 MeV which is consistent with the assumption that the activity is produced by the  $^{243}\text{Am} (^{13}\text{C}, 5n)^{251}\text{Md}$  reaction.<sup>6</sup> Unfortunately, no bombardments were performed with energies higher than 88 MeV. One can only assume that the excitation curve for the 7.75-MeV activity reaches

its maximum at about 88 MeV which would be in agreement with Sikkeland's calculations<sup>6</sup> for the  $^{243}\text{Am}(^{13}\text{C}, 6n)^{250}\text{Md}$  reaction. The fact that in both Fig. 4a and Fig. 4b the excitation curves for the 7.44-MeV activity have the same shape and apparently reach their maxima at the same energy as the excitation function for the 7.75-MeV activity support the assignment of the 7.44-MeV activity to the daughter of the 7.75-MeV activity. There were only two useful measurements for the excitation curve of the 7.04-MeV daughter activity. In Fig. 4b the two points are presented as open circles. Their relative values are consistent with the parent activity being produced by the  $^{243}\text{Am}(^{13}\text{C}, 4n)^{252}\text{Md}$  reaction.

The  $\alpha$  activities assigned to  $^{250}\text{Md}$  and  $^{251}\text{Md}$  were also produced by bombarding a  $^{243}\text{Am}$  target with  $^{12}\text{C}$  ions. The spectra were closely related to those in Figs. 1 and 2. The main differences were the appearance of a 7.31-MeV activity in parent spectra and the almost complete disappearance of the 7.04-MeV activity in daughter spectra. The latter was explained by the relatively small cross section of the  $(^{12}\text{C}, 3n)$  reaction at this energy. The 7.31-MeV activity belonged to  $^{247}\text{Es}$  which was predominantly produced by the  $(^{12}\text{C}, \alpha 4n)$  reaction. Again, in daughter spectra the 7.44-MeV activity decayed with the same apparent half-life as the 7.75-MeV activity in parent spectra indicating a parent-daughter relationship.

Excitation curves for the activities in parent and daughter spectra from bombardments of  $^{243}\text{Am}$  with  $^{12}\text{C}$  ions are presented in Fig. 5. Black circles mark the yield for the 7.55-MeV peak which has two sources. The excitation curve for the first activity contributing to the peak reaches its maximum at 71 MeV and supports the assumption that the activity is produced

by the  $^{243}\text{Am}(^{12}\text{C}, 4n)^{251}\text{Md}$  reaction. The second activity is  $^{249}\text{Fm}$  produced both as the electron-capture daughter of  $^{249}\text{Md}$  and by the  $(^{12}\text{C}, p5n)$  reaction. The 7.75-MeV peak is also composed of two activities. The excitation curve for the first activity reaching its maximum at 81 MeV is consistent with the activity being produced by the  $(^{12}\text{C}, 5n)$  reaction. The shape of the curve was taken from the excitation curve of the 7.44-MeV daughter activity in Fig. 5b. Also, in Fig. 5a, the excitation curve for the 7.44-MeV activity has its maximum at 81 MeV. The behavior of these excitation curves is in accordance with the assignment of the 7.75-MeV, 52-sec activity to  $^{250}\text{Md}$ . The second activity contributing to the 7.75-MeV peak is  $^{245}\text{Es}$ , the  $\alpha$ -decay daughter of the 8.03-MeV, 24-sec activity assigned to  $^{249}\text{Md}$ . The excitation curve for the 8.03-MeV activity reaches a maximum at about 91 MeV, which is taken as evidence that the activity is a product of the  $^{243}\text{Am}(^{12}\text{C}, 6n)^{249}\text{Md}$  reaction. In the daughter spectra there is a 7.73-MeV activity assigned to  $^{245}\text{Es}$ , which apparently decays with the same 24-sec half-life as the 8.03-MeV activity in parent spectra. As seen in Fig. 5b the excitation curve for this activity also reaches its maximum at about 91 MeV and gives further proof for a parent-daughter relationship between the 8.03-MeV and the 7.73-MeV activities. In Fig. 5a, the excitation curve for  $^{247}\text{Es}$  has a maximum at about 85 MeV, a value expected for the  $(^{12}\text{C}, \alpha 4n)$  reaction.

The  $\alpha$ -activities assigned to  $^{250}\text{Md}$  and  $^{251}\text{Md}$  were also produced by bombarding a  $^{240}\text{Pu}$  target with  $^{15}\text{N}$  ions. From data taken at only two bombardment energies, we concluded that the 7.55-MeV, 4-min  $\alpha$ -activity

belongs to a heavier isotope of Md than the 7.75-MeV, 52-sec  $\alpha$ -activity.

In our study of Lr isotopes,<sup>2</sup> tentative evidence was obtained for the 7.55-MeV, 4-min  $\alpha$ -activity to be the daughter of  $^{255}\text{Lr}$ .

## 2. $^{248}\text{Md}$ and $^{249}\text{Md}$

In bombardments of the  $^{241}\text{Am}$  target with  $^{12}\text{C}$  ions two new  $\alpha$  activities were observed: a 8.32-MeV, 7-sec activity assigned to  $^{248}\text{Md}$ , and a 8.03-MeV, 24-sec activity which was also observed in bombardments of  $^{243}\text{Am}$  with  $^{12}\text{C}$  ions and which was assigned to  $^{249}\text{Md}$ . The  $\alpha$ -particle spectra displayed in Fig. 8 were combined from four bombardments of  $^{241}\text{Am}$  with 75 to 91-MeV  $^{12}\text{C}$  ions and were recorded by the movable detectors while facing the wheel. The energies and relative intensities of the  $\alpha$ -particle groups were determined with the help of the SAMPO computer program.<sup>3</sup> The 7.136-MeV peak of  $^{214}\text{Ra}$  and the 8.03-MeV peak of the new isotope  $^{249}\text{Md}$  were used for shape calibration. The latter peak was chosen because the other  $\alpha$ -particle groups were either too weak or had too strong a contribution from nearby  $\alpha$ -particle groups. The energy value of 8.03-MeV for  $^{249}\text{Md}$  was chosen to give correct energies for the known  $\alpha$ -particle groups.

$^{248}\text{Md}$  has a similar complex  $\alpha$ -particle spectrum as  $^{250}\text{Md}$ . Besides the 8.32-MeV main  $\alpha$ -particle group (~ 75%) there is another group (~ 25%) at about 8.36 MeV.  $^{248}\text{Fm}$  is present in the spectra mainly as the electron-capture daughter of  $^{248}\text{Md}$ . The 7.73-MeV  $\alpha$ -particle group is predominantly due to  $^{245}\text{Es}$ , which is produced partly by the ( $^{12}\text{C}$ ,  $\alpha 4n$ ) reaction and partly as the  $\alpha$ -decay daughter of  $^{249}\text{Md}$ . A small fraction (<3%) of the 7.73-MeV  $\alpha$ -particle group is due to  $^{250}\text{Md}$ . The 7.36-MeV activity belongs to  $^{246}\text{Es}$  which is produced by the ( $^{12}\text{C}$ ,  $\alpha 3n$ ) reaction. Most of the 7.21-MeV  $^{244}\text{Cf}$  is produced directly in bombardments, although some of it is present as a descendant

of  $^{248}\text{Md}$  and  $^{244}\text{Es}$ . The longer-lived component in the 7.14-MeV  $\alpha$ -particle group belongs to  $^{245}\text{Cf}$ , the EC daughter of  $^{245}\text{Es}$ . The origin of the other  $\alpha$ -particle groups was explained in the connection with Fig. 1.

The combined spectra recorded by the same detectors as in Fig. 6 but in the off-wheel position, and by the stationary detectors facing them, are shown in Fig. 7. The 6.757-MeV peak of  $^{246}\text{Cf}$  and the 7.87-MeV peak of  $^{248}\text{Fm}$  were used for calibration. The  $^{248}\text{Fm}$  peak seems to decay with the same half-life as the 8.32-MeV peak in the parent spectra (Fig. 6) supporting the assignment of the 8.32-MeV activity to  $^{248}\text{Md}$ . The  $\alpha$ -decay daughter of  $^{248}\text{Md}$ ,  $^{244}\text{Es}$ , is not seen in the spectra because it has been found to decay predominantly by electron capture.<sup>7</sup> However, the granddaughter of  $^{248}\text{Md}$ , the 7.21-MeV  $^{244}\text{Cf}$ , is clearly visible. It is mostly produced via  $^{248}\text{Md} \xrightarrow{\text{EC}} ^{248}\text{Fm} \xrightarrow{\alpha} ^{244}\text{Cf}$ . For  $^{249}\text{Md}$  both the  $\alpha$ -decay daughter, the 7.73-MeV  $^{245}\text{Es}$ , and the electron-capture daughter, the 7.54-MeV  $^{249}\text{Fm}$ , are seen in Fig. 7. Also the granddaughter of  $^{249}\text{Md}$ , the 7.14-MeV  $^{245}\text{Cf}$ , is present in the spectra.  $^{250}\text{Fm}$ , the electron-capture daughter of  $^{250}\text{Md}$ , has an apparent half-life of about 10 sec instead of 50 sec. This is because the  $^{250}\text{Fm}$  activity was mainly residue from previous experiments where the wheel-stepping interval was 20 sec instead of 4 sec.

Further support of the mass assignments given to the Md isotopes was obtained from excitation function studies. The excitation curves in Fig. 8a are for the activities in parent spectra and those in Fig. 8b for the daughter activities produced in bombardments of  $^{241}\text{Am}$  with  $^{12}\text{C}$  ions. In Fig. 8a the excitation curves for the 8.03- and 8.32-MeV activities reach their maxima at about 72 and 81 MeV, respectively, which is consistent with the activities being produced by  $^{241}\text{Am}(^{12}\text{C}, 4n)^{249}\text{Md}$  and  $^{241}\text{Am}(^{12}\text{C}, 5n)^{248}\text{Md}$  reactions,<sup>6</sup> respectively. In Fig. 8b, the excitation curves for  $^{245}\text{Es}$  and  $^{249}\text{Fm}$  indicate that the 8.03-MeV activity is a precursor for both of them, and the excitation curve for  $^{248}\text{Fm}$

supports the parent-daughter relationship between the 8.32-MeV activity and  $^{248}\text{Fm}$ . In Fig. 8a, the excitation curve for  $^{245}\text{Es}$  has been split into two components, because  $^{245}\text{Es}$  is present both as the daughter of  $^{249}\text{Md}$  and as a result of the  $(^{12}\text{C}, \alpha n)$  reaction. The shape of the former component has been assumed to be the same as that of the excitation curve for the 8.03-MeV activity. However, at the lowest bombarding energy, 66.5 MeV, the 7.73-MeV activity is mainly due to  $^{250}\text{Md}$  produced by the  $(^{12}\text{C}, 3n)$  reaction. At higher energies the contribution of  $^{250}\text{Md}$  to this component is of the order of 10%. The second component reaching its maximum at about 85 MeV is in accordance with the activity being produced by the  $(^{12}\text{C}, \alpha n)$  reaction.

In their study of Es isotopes Mikheev et. al.,<sup>5</sup> reported the same  $\alpha$ -particle energy value of  $7.33 \pm 0.03$  MeV for both  $^{246}\text{Es}$  and  $^{247}\text{Es}$ . In the present work the  $\alpha$ -particle energy of  $^{246}\text{Es}$  was measured to be  $7.36 \pm 0.03$  MeV and that of  $^{247}\text{Es}$ ,  $7.31 \pm 0.03$  MeV. The activities were produced by  $^{241}\text{Am}(^{12}\text{C}, \alpha 3n)^{246}\text{Es}$  and  $^{241}\text{Am}(^{12}\text{C}, \alpha 2n)^{247}\text{Es}$  reactions. The 50-keV difference in energy values made it possible to get separate excitation functions, presented in Fig. 8a, for these activities. The separation was done manually using the shape of the 7.136-MeV  $^{214}\text{Ra}$  peak for shape calibration.

### 3. Half-Life Information

The half-life of  $^{252}\text{Md}$  was discussed earlier in Sec. III-1. The decay curves for the other Md isotopes studied in this work are presented in Fig. 9. Open circles are used for the parent  $\alpha$  activity to mark the number of counts at each of the seven detector stations recorded by the movable detectors when facing the wheel; the closed circles for the daughter  $\alpha$  activity show the number of counts recorded by the same detectors when in the off-wheel position combined with the counts recorded by the stationary detectors facing

them. The parent-daughter pair involved in each case is indicated on top of each section of Fig. 9. In Fig. 9a the same spectra as in Figs. 6 and 7 were used. By quadrants of the 120-sec shuttle period, the daughter counts are distributed as 53, 26, 8 and 3 giving a half-life of  $24 \pm 7$  sec for the daughter. This half-life is somewhat shorter than the reported value of  $38 \pm 4$  sec<sup>8</sup> for  $^{248}\text{Fm}$ . The data points in Fig. 9b are based on a series of bombardments of  $^{241}\text{Am}$  with  $^{12}\text{C}$  ions. The distribution of daughter counts by quadrants of the 120-sec shuttle period is 40, 29, 20, and 16, which gives a half-life of  $65 \pm 35$  sec for the daughter. This half-life is in accordance with the reported value<sup>5</sup> of  $1.33 \pm 0.15$  min for  $^{245}\text{Es}$ . The decay curves in Figs. 9c and 9d are based on bombardments of  $^{243}\text{Am}$  with  $^{12}\text{C}$  ions. In Fig. 9c, the distribution of the daughter counts by quadrants of the 12-min shuttle period is 127, 125, 93 and 93, which gives a daughter half-life of  $17 \pm 12$  min for the 30-min  $^{250}\text{Fm}$ . Because both the  $\alpha$ -decay and the EC daughter of  $^{251}\text{Md}$  mainly undergo EC themselves<sup>5,4</sup> it was not possible to obtain a daughter decay curve in Fig. 9d. From the same spectra as used for Fig. 9d a half-life value of  $4.7 \pm 0.3$  min was derived for  $^{247}\text{Es}$ .

#### 4. Electron Capture Branching Ratios

In order to get estimates for the EC branching of Md isotopes, it was necessary to determine the transfer efficiency  $\epsilon_r$  of the EC daughter atoms onto the detectors relative to that of the  $\alpha$ -decay recoils. This was done by comparing the ratio of EC-daughter counts in daughter and parent spectra  $(D/DP)_{\text{EC}}$  to the calculated ratio  $(D/DP)_{100\%}$ , where  $\epsilon_r$  was assumed to be 100%. In  $^{243}\text{Am}$  bombardments, where the wheel was biased negatively by 10V relative to the detectors, the value  $\epsilon_r = 15\%$  was obtained for  $^{250}\text{Fm}$  recoils. In all  $^{241}\text{Am}$  bombardments the wheel was biased positively by 10V but the timing conditions

were such that the ratio  $(D/DP)_{100\%}$  could not be calculated accurately. However, in an experiment, where a  $^{243}\text{Am}$  target was bombarded by  $^{13}\text{C}$  ions and a bias voltage of +10V was applied, it was found that  $\epsilon_r$  for  $^{250}\text{Fm}$  recoils increased by a factor of two relative to the case of -10V bias voltage. Accordingly, a value  $\epsilon_r = 30\%$  was assumed for the  $^{248}\text{Fm}$  recoils in  $^{241}\text{Am}$  bombardments.

By comparing the experimental ratio  $(D/P)_{\text{EC}}$  with the calculated ratio  $(D/P)_{100\%}$  (D = number of Fm-daughter counts in daughter spectra, P = number of Md-parent counts in parent spectra) and using the values  $\epsilon_r = 15\%$  and  $\epsilon_r = 30\%$ , respectively, values of  $94 \pm 3\%$  and  $80 \pm 10\%$  were obtained for EC branchings of  $^{250}\text{Md}$  and  $^{248}\text{Md}$ . The EC branchings of  $^{251}\text{Md}$  and  $^{249}\text{Md}$  could not be derived in the same fashion, because the  $\alpha$ -decay branchings of  $^{251}\text{Fm}$  and  $^{249}\text{Fm}$  are small and poorly known (about 1% for  $^{251}\text{Fm}$  and unreported for  $^{249}\text{Fm}$ ). However, coarse estimates can be made on the basis of observed reaction cross sections. In Fig. 4a, the maxima of the excitation curves for  $^{251}\text{Md}$  and  $^{250}\text{Md}$  correspond to absolute cross sections of 160nb and 50nb, respectively. By comparing the ratio of these values to the ratio of measured (HI, 5n)- and (HI, 6n)-reaction cross sections for Cf and Lr isotopes<sup>9,2</sup> it can be deduced that the EC branching of  $^{251}\text{Md}$  is about the same or higher than that of  $^{250}\text{Md}$ . If both isotopes had the same EC branching of 94%, the cross section of  $^{243}\text{Am} (^{13}\text{C}, 5n) ^{251}\text{Md}$  reaction would be 2.7  $\mu\text{b}$  and that of  $^{243}\text{Am} (^{13}\text{C}, 6n) ^{250}\text{Md}$  reaction 0.76  $\mu\text{b}$ . A similar comparison between the cross sections for  $^{249}\text{Md}$  and  $^{248}\text{Md}$  in Fig. 8a and the measured (HI, 4n)- and (HI, 5n)-reaction cross sections for Cf and No isotopes<sup>9,10</sup> leads to a conclusion that the EC branching of  $^{249}\text{Md}$  is about the same or less than that of  $^{248}\text{Md}$ . If the EC branching were the same (80%) for both isotopes, the cross section of  $^{241}\text{Am} (^{12}\text{C}, 4n) ^{249}\text{Md}$  reaction

would be 0.42  $\mu\text{b}$  and that of  $^{241}\text{Am}(^{12}\text{C}, 5\text{n})^{248}\text{Md}$  reaction 0.07  $\mu\text{b}$ . With the above assumptions, in bombardments of a  $^{243}\text{Am}$  target with  $^{12}\text{C}$  ions (Fig. 5a) the cross sections for 4n, 5n, and 6n reactions would be 2.8, 1.4, and 0.55  $\mu\text{b}$ , respectively.

On the basis of the excitation functions shown in Fig. 8 it is possible to get an estimate for the EC branching of  $^{245}\text{Es}$ . If  $^{245}\text{Es}$  did not decay by EC at all, the maxima of the excitation curves of  $^{249}\text{Md}$  in Fig. 8a and  $^{245}\text{Es}$  in Fig. 8b should have the same value. Since the maximum value of the  $^{245}\text{Es}$  excitation curve is about 40% of the maximum value of the  $^{249}\text{Md}$  excitation curve, the EC branching  $^{245}\text{Es}$  is about 60%. This is considerably smaller than the value  $83\pm\frac{4}{3}\%$  reported by Mikheev et. al.<sup>5</sup>

#### IV. DISCUSSION

The experimental results obtained in this study are summarized in Table I. The half-life values are mostly averages from several bombardments or series of bombardments. In each case the half-life was determined by a least-squares analysis, with error limits set equal to twice the standard deviation of the fit. Thus the error estimates for the half-lives given in Table I are consistent with each other. The contribution of systematic errors was difficult to estimate, but it was expected to be small compared to that of statistical errors. In the case of the  $\alpha$ -particle energies the uncertainty is mostly caused by calibration errors. The peaks used for calibration were mentioned in connection with each spectrum in Section III. Equalizing the gains and thresholds in all of the 28 detectors was done prior to an experiment using pulse generators calibrated by the 6.640-MeV  $\alpha$ -particle group of  $^{253}\text{Es}$  samples. Further gain matching of the spectra was done during the data handling phase of the CDC 6600 computer using Paatero's method.<sup>11</sup>

The  $\alpha$ -decay hindrance factors were calculated using the spin-independent ( $l=0$ ) equations of Preston.<sup>12</sup> This formalism was chosen because it is widely used and thus facilitates the comparisons with hindrance factors calculated by others. The radius parameter  $R$  was chosen to decrease from 9.45 fm for  $^{248}\text{Md}$ , in 0.05-fm decrements, to 9.30 fm for  $^{251}\text{Md}$ . The choice was based on the general trend among the  $R$  values for even-even Cf and Fm  $\alpha$ -emitters with neutron number less than 152. In the hindrance factor calculations the values 80% and 94% were used for the EC branchings of  $^{249}\text{Md}$  and  $^{251}\text{Md}$ , respectively. The hindrance factors of the main  $\alpha$ -particle groups of  $^{249}\text{Md}$ ,  $^{250}\text{Md}$ , and  $^{251}\text{Md}$  indicate that the transitions are favored.

$\alpha$ -decay energies of the heaviest elements as a function of neutron number are plotted in Fig. 10. This figure was already presented in our paper on Lr isotopes.<sup>2</sup> The present data on  $\alpha$ -decay energies of Md isotopes were previewed in that paper and some systematic features were indicated. In Fig. 10, the black circles either correspond to the most energetic known  $\alpha$ -particle group or mark the values estimated by Wapstra et al.<sup>13</sup> with errors less than 40 keV, the open circles mark estimated values based on systematics (cf. Fig. 4 in Ref. 13). For Md isotopes both the experimental and the estimated values have been plotted to show that the observed  $\alpha$ -decay energies are consistently lower than the estimated ones by some 300 keV. The only exceptions are  $^{255}\text{Md}$ , where a  $\gamma$ -ray of energy  $430 \pm 40$  keV was identified in coincidence with the main  $\alpha$ -particle group,<sup>14</sup> and  $^{256}\text{Md}$ , where a weak  $\alpha$ -particle group has been observed with an energy that agrees with the estimate.<sup>15</sup> This phenomenon can be understood in terms of the single-particle level scheme of Nilsson et. al.<sup>16</sup> According to the scheme there is a fairly large gap between the  $7/2^-$  [514 $\uparrow$ ] state available for the 101st proton and the  $7/2^+$  [633 $\uparrow$ ] state available for the 99th proton.  $\alpha$ -decay from the  $7/2^-$  [514 $\uparrow$ ] state, the

predicted ground state of odd Md isotopes, to the  $7/2^+[633\uparrow]$  state, the ground state of odd Es isotopes, is greatly hindered because of a change of both parity and relative orientation of the projection of intrinsic spin.<sup>17</sup> Therefore the favored alpha decay from the  $7/2^-[514\downarrow]$  state of Md to the same state in Es is much preferred even if the level in the latter lies several hundreds of keV above the ground state.

Log-ft values of the EC transitions can be estimated by using the observed half-life values and the EC-decay energies from the binding-energy systematics of Wapstra et. al.<sup>13</sup> for  $^{252}\text{Md}$ ,  $^{251}\text{Md}$ , and  $^{250}\text{Md}$ , and extrapolated values for  $^{249}\text{Md}$  and  $^{248}\text{Md}$ . The log-ft values between 4.5 and 5.4 which were obtained for these isotopes are unusually low for the heavy element region and thus difficult to explain in terms of the single-particle level scheme of Nilsson et. al.

I am greatly indebted to my colleagues Albert Ghiorso, Matti Nurmiä, and Kari Eskola for their kind and extensive cooperation in carrying out the experiments. Also, I want to express my appreciation of the expert help given by the HILAC crew.

REFERENCES

† AEC Contract No W-7405-eng-48

This work was performed under the auspices of the U.S. Atomic Energy Commission.

1. E. D. Donets, V. A. Schegolev, and V. A. Ermakov, *Yadern. Fiz.* 2 1015 (1965) [transl.: *Soviet J. Nucl. Phys.* 2, 723 (1966)].
2. K. Eskola, P. Eskola, M. Nurmi, and A. Ghiorso, *Phys. Rev. C* 4, 632 (1971).
3. J. T. Routti and S. G. Prussin, *Nucl. Instr. Methods* 72, 125 (1969).
4. S. Amiel, A. Chetham-Strode, Jr., G. R. Choppin, A. Ghiorso, B. G. Harvey, L. W. Holm, and S. G. Thompson, *Phys. Rev.* 106, 553 (1957).
5. V. L. Mikheev, V. I. Ilyushchenko, and M. B. Miller, *Yadern. Fiz.* 5, 49 (1967) [transl.: *Soviet J. Nucl. Phys.* 5, 35 (1967)].
6. T. Sikkeland and D. F. Lebeck, unpublished.
7. P. Eskola, University of California Radiation Laboratory Report No. UCRL-20426, 35, 1971 (unpublished).
8. M. Nurmi, T. Sikkeland, R. Silva, and A. Ghiorso, *Phys. Letters* 26B, 78 (1967).
9. T. Sikkeland, J. Maly, and D. F. Lebeck, *Phys. Rev.* 169, 1000 (1968).
10. T. Sikkeland, A. Ghiorso, and M. Nurmi, *Phys. Rev.* 172, 1232 (1968).
11. P. Paatero, *Nucl. Instr. Methods* 31, 360 (1964).
12. M. A. Preston, *Phys. Rev.* 71, 865 (1946).
13. A. E. Wapstra, C. Kurzeck, and A. Anisimoff, in *Proceedings of the Third International Conference on Atomic Masses, Winnipeg, Canada, 1967*, edited by R. C. Barber (University of Manitoba Press, Winnipeg, Canada, 1967), p. 153.
14. P. R. Fields, I. Ahmad, R. F. Barnes, R. K. Sjoblom, and E. P. Horwitz, *Nucl. Phys.* A154, 407 (1970).
15. R. W. Hoff, E. K. Hulet, R. J. Dupzyk, R. W. Lougheed, and J. E. Evans, *Nucl. Phys.* A169, 641 (1971).
16. S. G. Nilsson, C. F. Tsang, A. Sobiczewski, Z. Szymanski, S. Wycech, C. Gustafson, I.-L. Lamm, P. Möller, and B. Nilsson, *Nucl. Phys.* A131, 1 (1969).
17. O. Prior, *Arkiv för Fysik* 16, 15 (1959).

Table I. Summary of experimental results.

	Half-life	$\alpha$ -particle energy (MeV)	Intensity (%)	$\frac{EC}{\alpha+EC}$ (%)	$\alpha$ -decay hindrance factor	Ways of production
$^{248}\text{Md}$	$7 \pm 3$ sec	$8.32 \pm 0.02$	$\sim 75$	$80 \pm 10$	22	$^{241}\text{Am} + ^{12}\text{C}$
		$8.36 \pm 0.03$	$\sim 25$		88	
$^{249}\text{Md}$	$24 \pm 4$ sec	$8.03 \pm 0.02$	100		$\approx 5$	$^{241}\text{Am} + ^{12}\text{C}$
						$^{243}\text{Am} + ^{12}\text{C}$
$^{250}\text{Md}$	$52 \pm 6$ sec	$7.75 \pm 0.02$	$\sim 70$	$94 \pm 3$	4	$^{240}\text{Pu} + ^{15}\text{N}$
		$7.82 \pm 0.03$	$\sim 30$		18	$^{241}\text{Am} + ^{16}\text{O}$
						$^{243}\text{Am} + ^{12}\text{C}, ^{13}\text{C}$
$^{251}\text{Md}$	$4.0 \pm 0.5$ min	$7.55 \pm 0.02$	100		$\approx 2$	$^{240}\text{Pu} + ^{15}\text{N}$
						$^{243}\text{Am} + ^{12}\text{C}, ^{13}\text{C}$
$^{252}\text{Md}$	$2.3 \pm 0.8$ min					
$^{245}\text{Es}$		$7.73 \pm 0.02$	100	$60 \pm 10$		$^{241}\text{Am} + ^{12}\text{C}$
$^{246}\text{Es}$		$7.36 \pm 0.03$	100			$^{241}\text{Am} + ^{12}\text{C}$
$^{247}\text{Es}$	$4.7 \pm 0.3$ min	$7.31 \pm 0.03$	100			$^{241}\text{Am} + ^{12}\text{C}$
						$^{243}\text{Am} + ^{12}\text{C}$

FIGURE CAPTIONS

- Fig. 1 A series of  $\alpha$ -particle spectra produced by a bombardment of  $^{243}\text{Am}$  with  $^{13}\text{C}$  ions. The individual spectra show the total of counts recorded at each of the seven stations by the two movable detectors when facing the wheel. The sum of the seven spectra is plotted topmost. These spectra are called the "parent" spectra. The wheel-stepping interval, the integrated beam reading, and the bombardment energy are indicated in the figure.
- Fig. 2 A series of  $\alpha$ -particle spectra resulting from the same bombardment of  $^{243}\text{Am}$  with  $^{13}\text{C}$  ions as the spectra in Fig. 1, but recorded by the detectors in the off-wheel position ("daughter" spectra). The arrangement of the spectra and the data pertinent to the bombardment correspond to those in Fig. 1. The seventh station was left out because of problems in adjusting the energy scale.
- Fig. 3 Decay of the 7.04-MeV  $\alpha$ -particle group of  $^{252}\text{Fm}$  in "daughter" spectra combined from four bombardments of  $^{243}\text{Am}$  with 72-88 MeV  $^{13}\text{C}$  ions. The error bars indicate an uncertainty of one standard deviation.
- Fig. 4 Excitation curves for some activities produced in bombardments of  $^{243}\text{Am}$  with  $^{13}\text{C}$  ions. The upper part displays the excitation curves for the activities in "parent" spectra and the lower part those for the activities in "daughter" spectra. The curves in Fig. 4b have been corrected for geometry and time factors to make them comparable with the curves in Fig. 4a. The error bars indicate an uncertainty of one standard deviation; where no error bars are marked the uncertainty is close to the size of the point showing the experimental result.
- Fig. 5 Excitation curves for some activities produced in the bombardments of  $^{243}\text{Am}$  with  $^{12}\text{C}$  ions. For further details see the caption of Fig. 4.

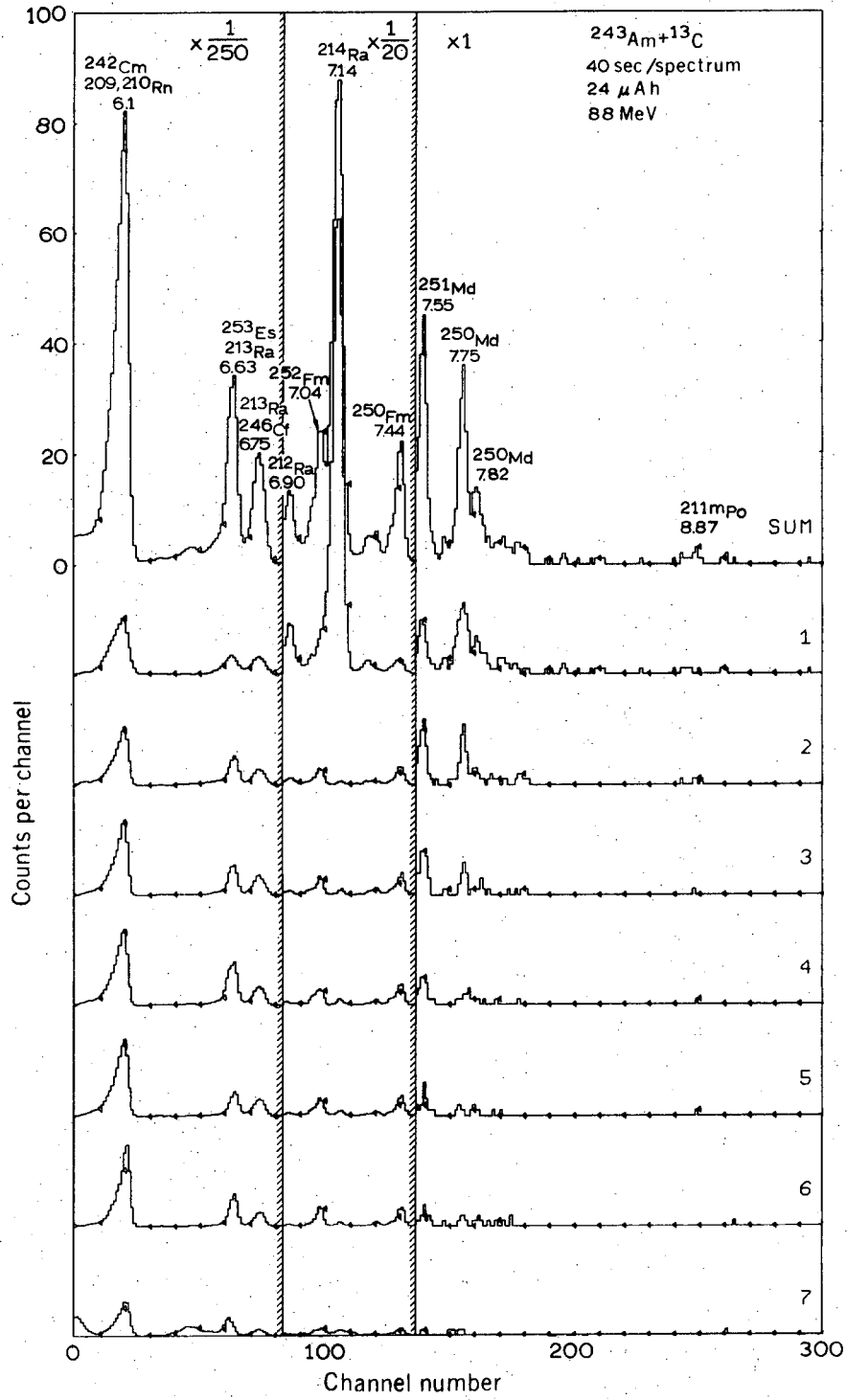
Fig. 6 A series of  $\alpha$ -particle "parent" spectra produced by bombardments of  $^{241}\text{Am}$  with  $^{12}\text{C}$  ions. Both the arrangement of the spectra and the data pertinent to the bombardments correspond to those in Fig. 1.

Fig. 7 A series of  $\alpha$ -particle "daughter" spectra resulting from the same bombardments of  $^{241}\text{Am}$  with  $^{12}\text{C}$  ions as the "parent" spectra in Fig. 6. Both the arrangement of the spectra and the data pertinent to the bombardment correspond to those in Fig. 1.

Fig. 8 Excitation curves for some activities produced in the bombardments of  $^{241}\text{Am}$  with  $^{12}\text{C}$  ions. For further details see the caption of Fig. 4.

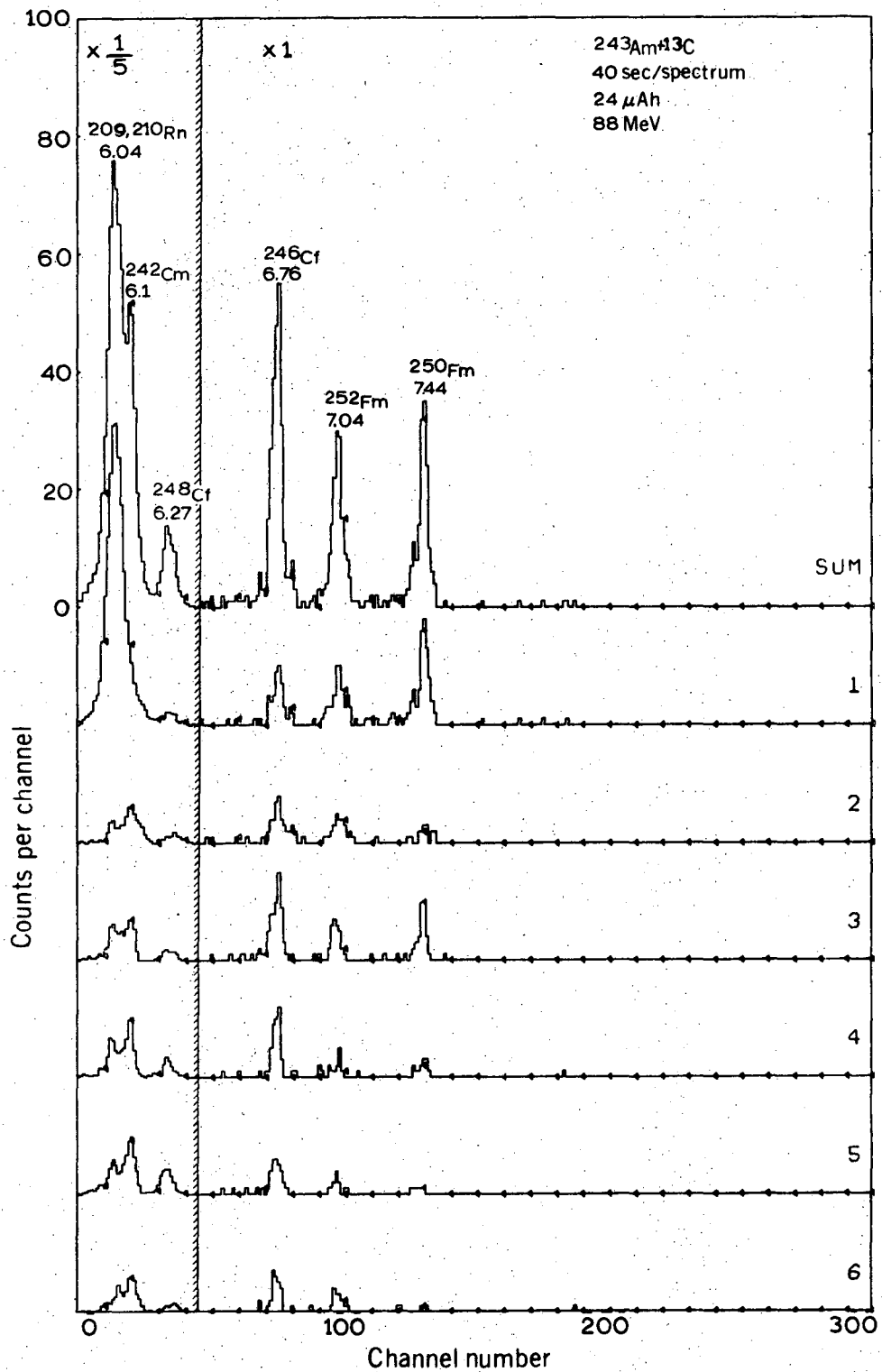
Fig. 9 Decay curves for  $\alpha$ -decay of  $^{248}\text{Md}$ ,  $^{249}\text{Md}$ ,  $^{250}\text{Md}$ , and  $^{251}\text{Md}$  in "parent" spectra and their daughter activities in corresponding "daughter" spectra. The parent-daughter pair involved in each case is written on top of each section. Open circles denote the parent  $\alpha$  activity, black circles the daughter  $\alpha$ -activity.

Fig. 10  $\alpha$ -decay energy as a function of neutron number. The black circles either correspond to the highest known  $\alpha$ -particle group or mark the values estimated by Wapstra et. al.<sup>13</sup> with errors less than 40 keV, the open circles mark estimated values based on systematics (cf. Fig. - in Ref. 13).



XBL 7111 2427

Fig. 1



XBL 7111 2429

Fig. 2

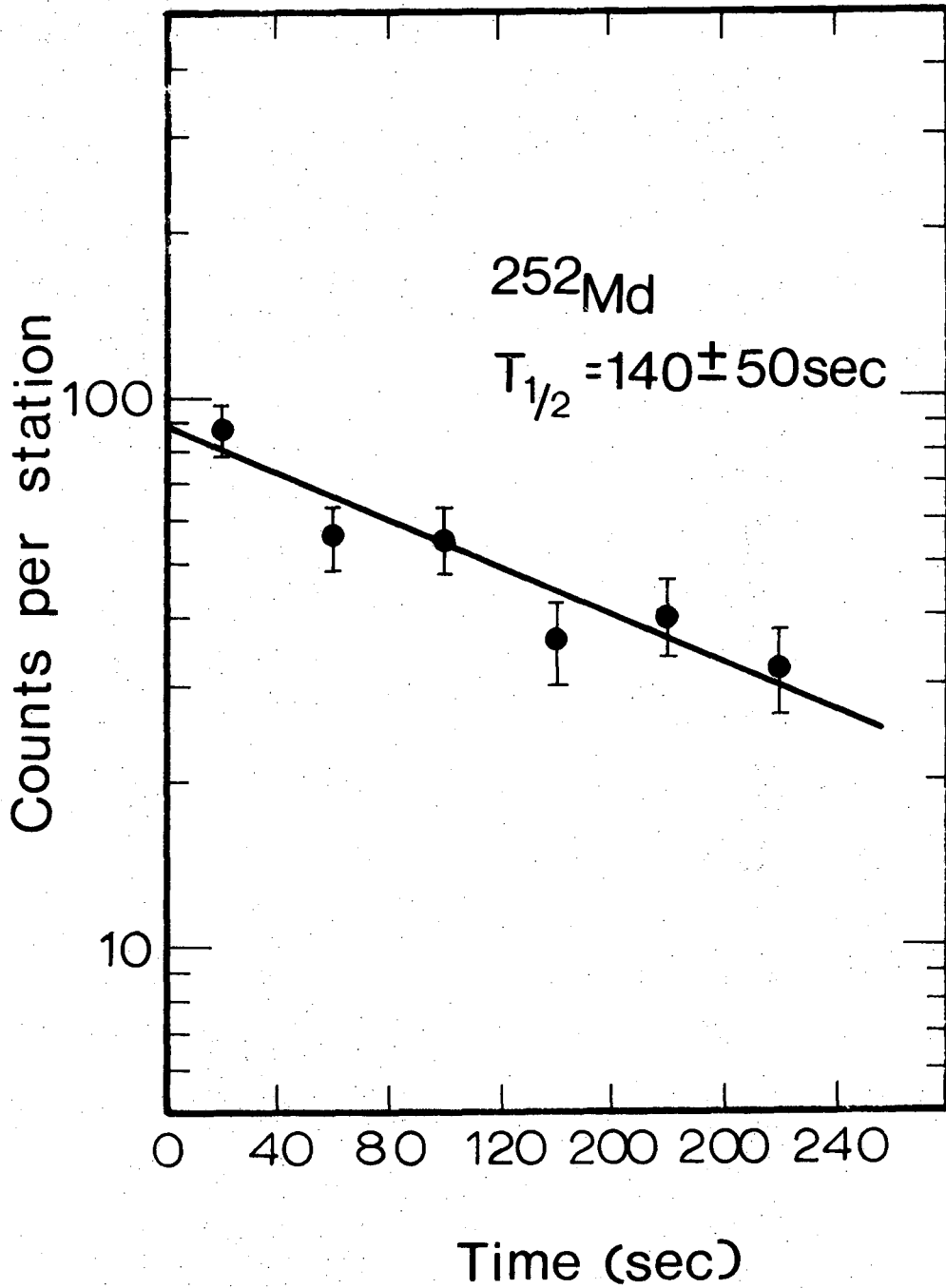


Fig. 3 XBL 723 5610

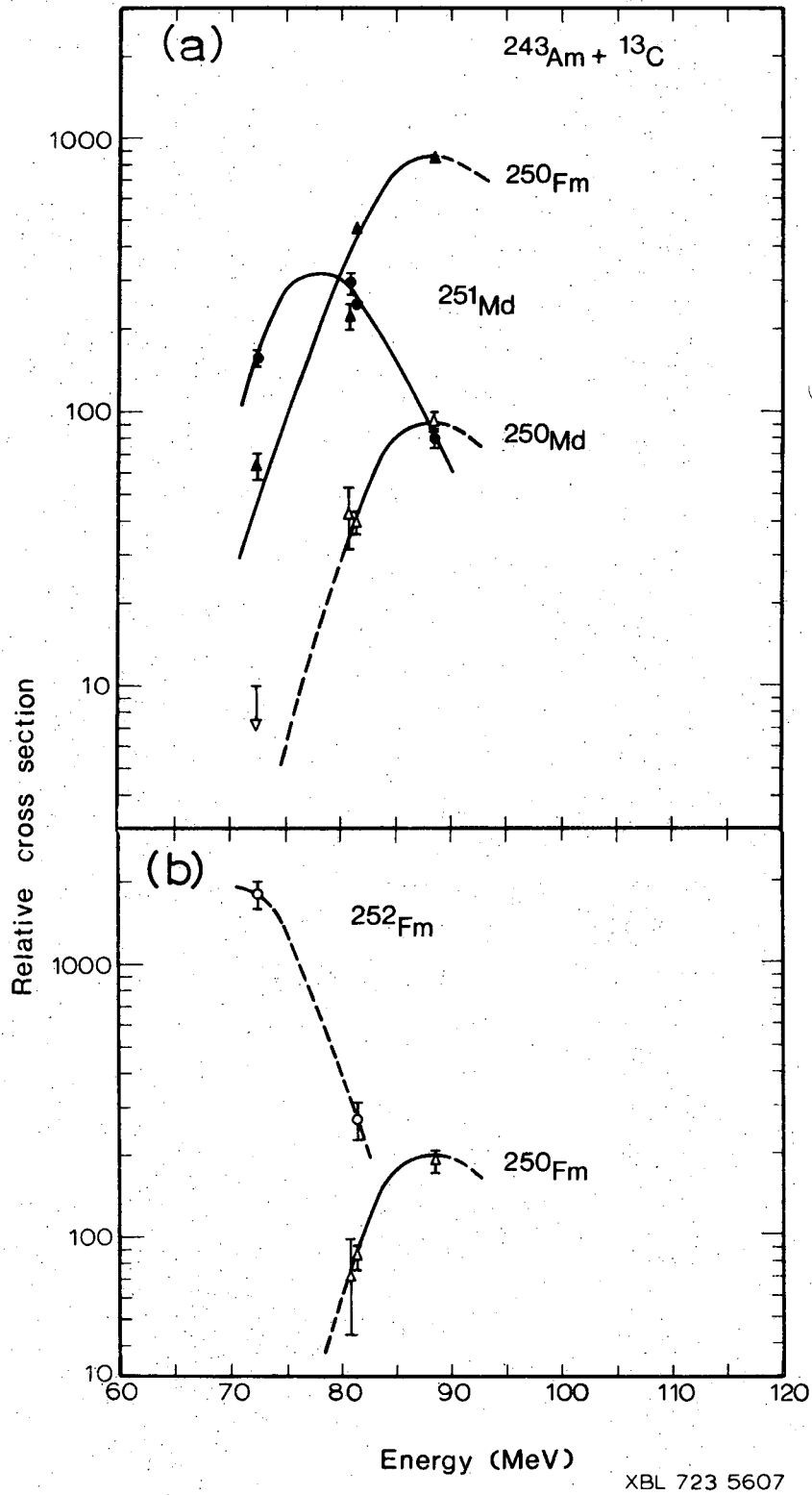
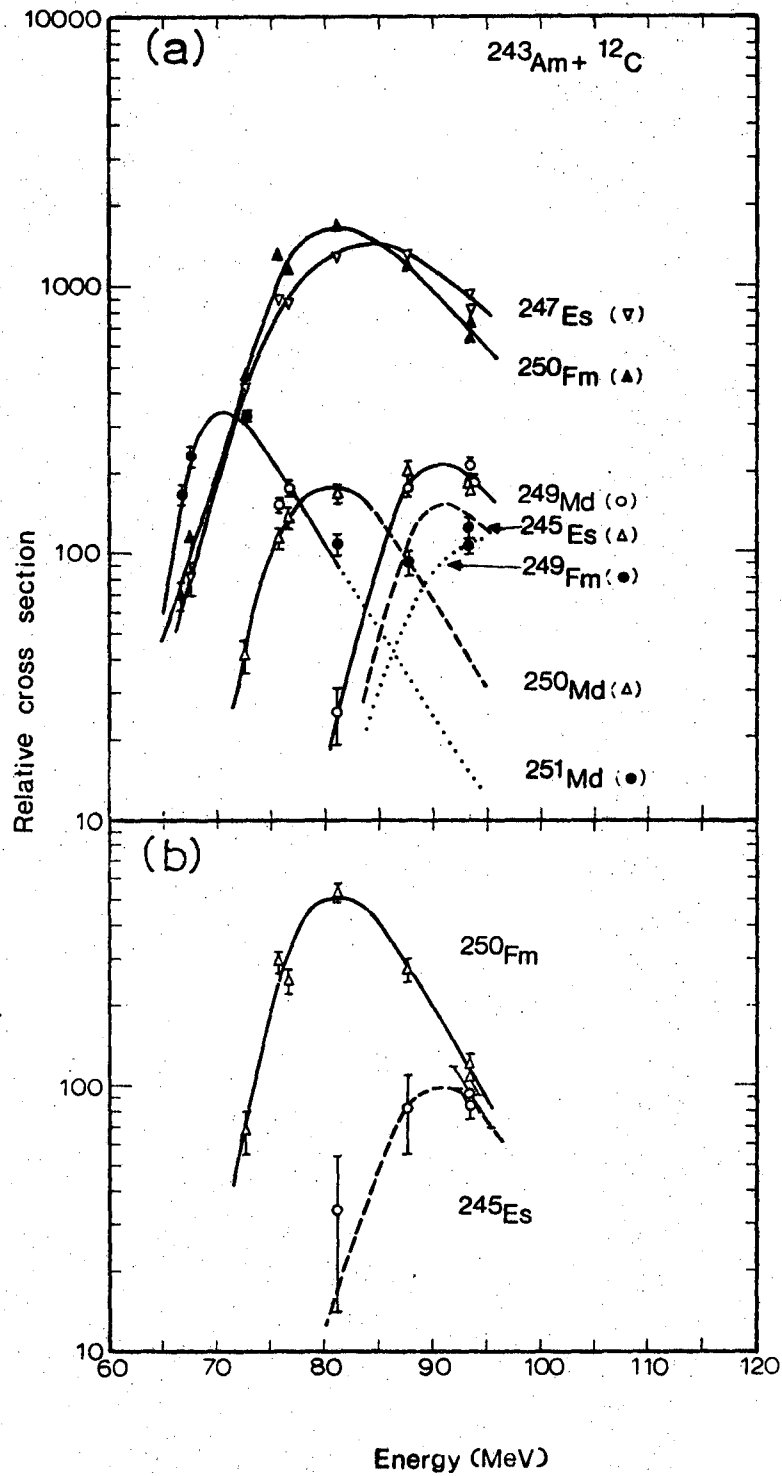
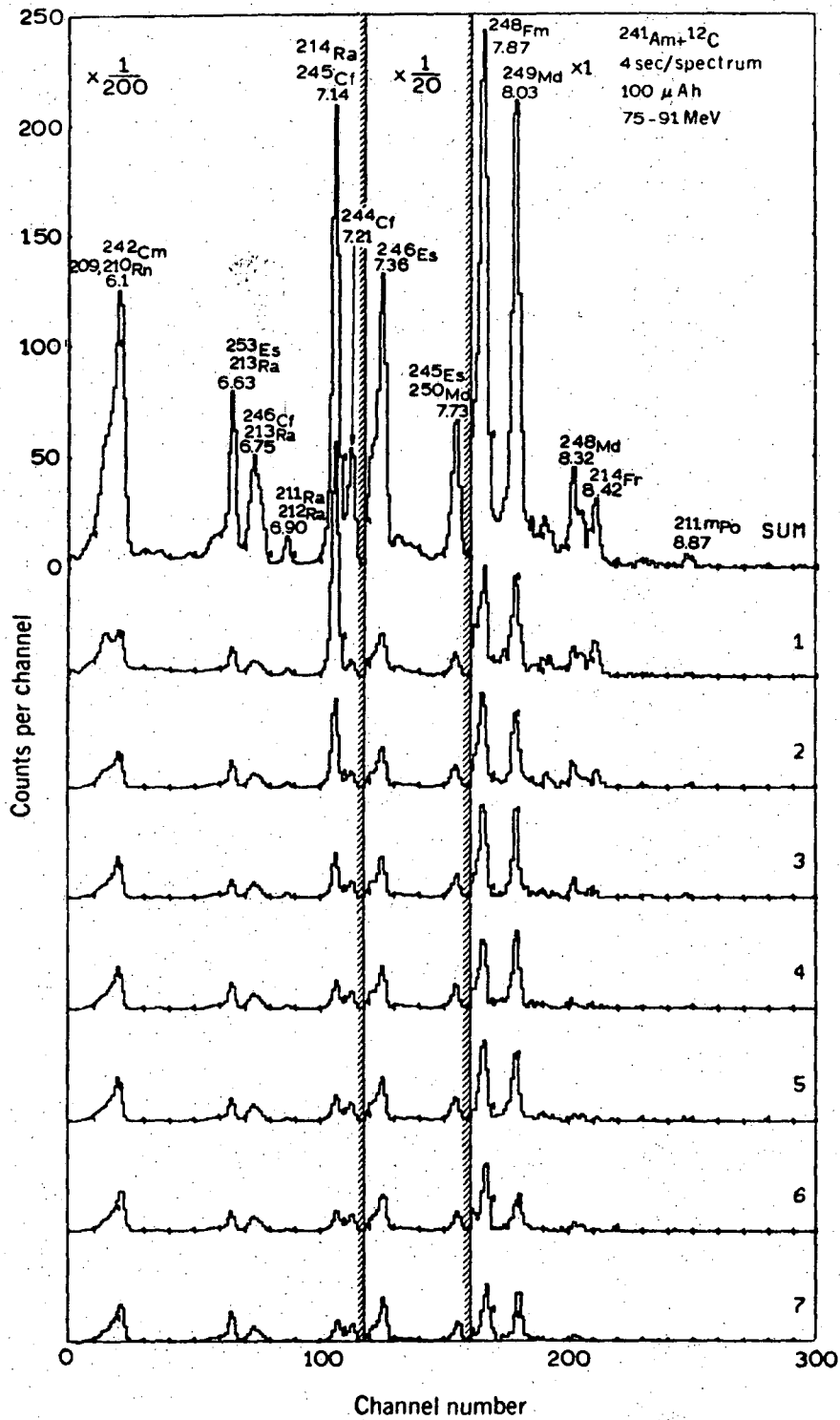


Fig. 4



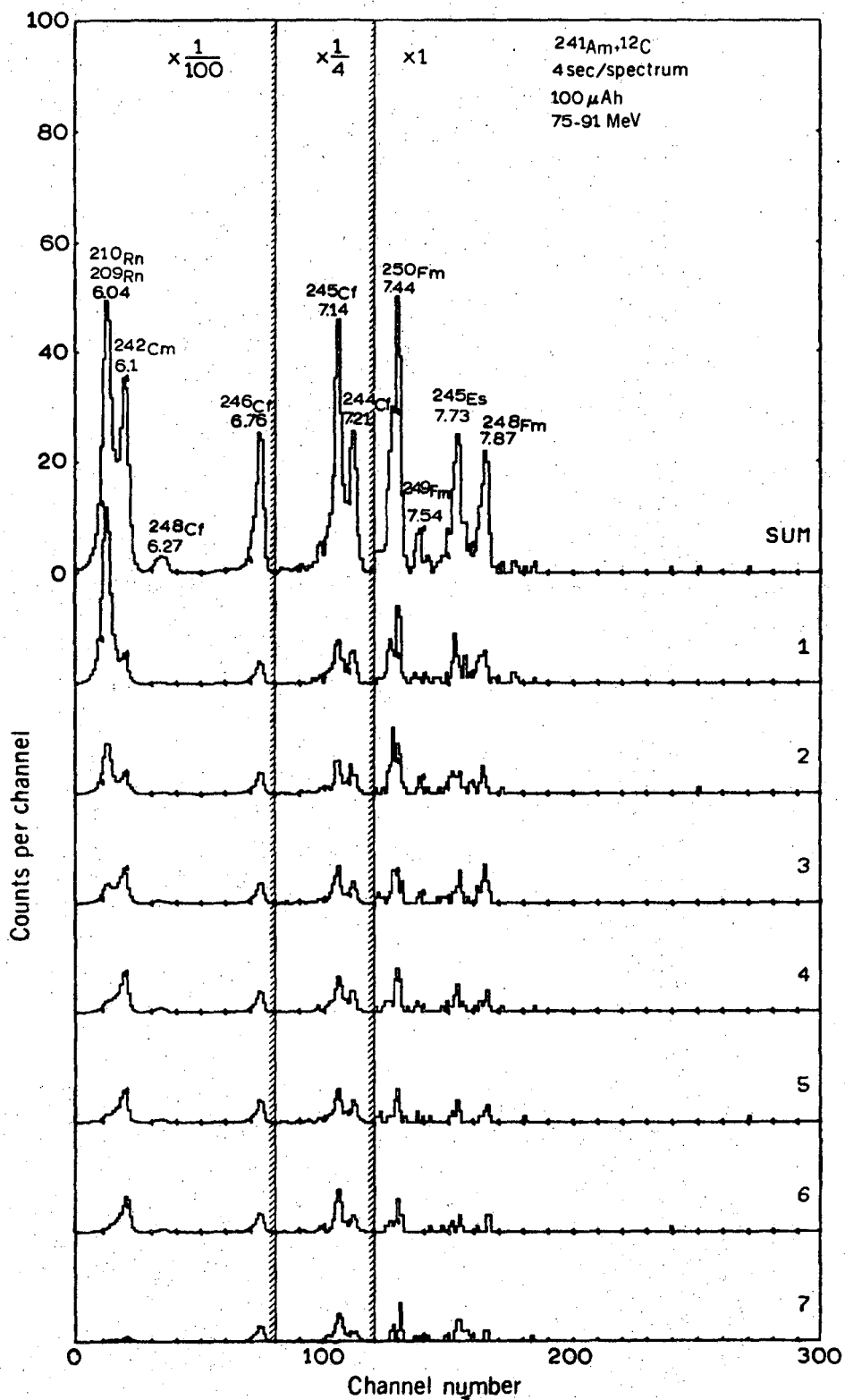
XBL 723 5608

Fig. 5



XBL 7111 2426

Fig. 6



XBL 7111 2430

Fig. 7

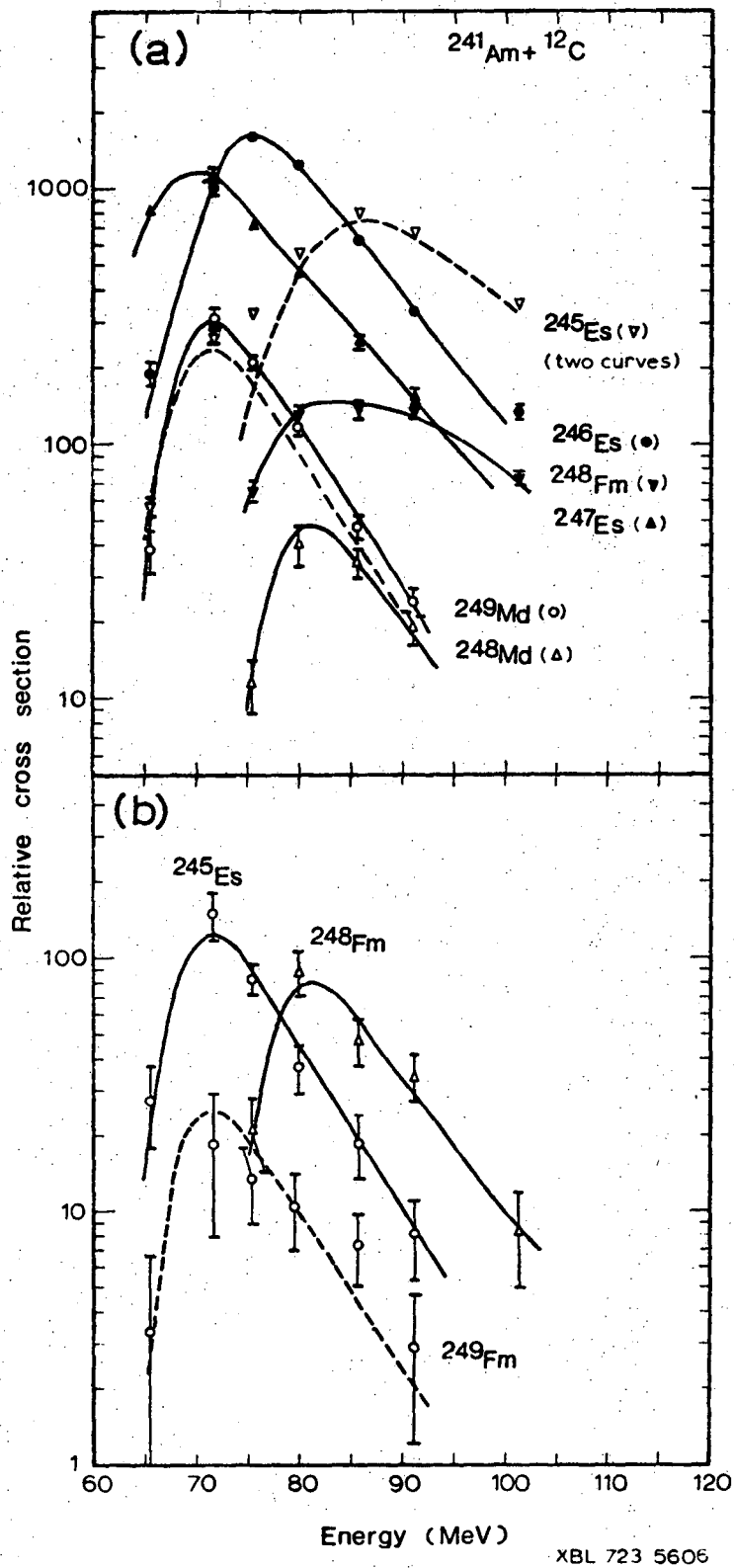
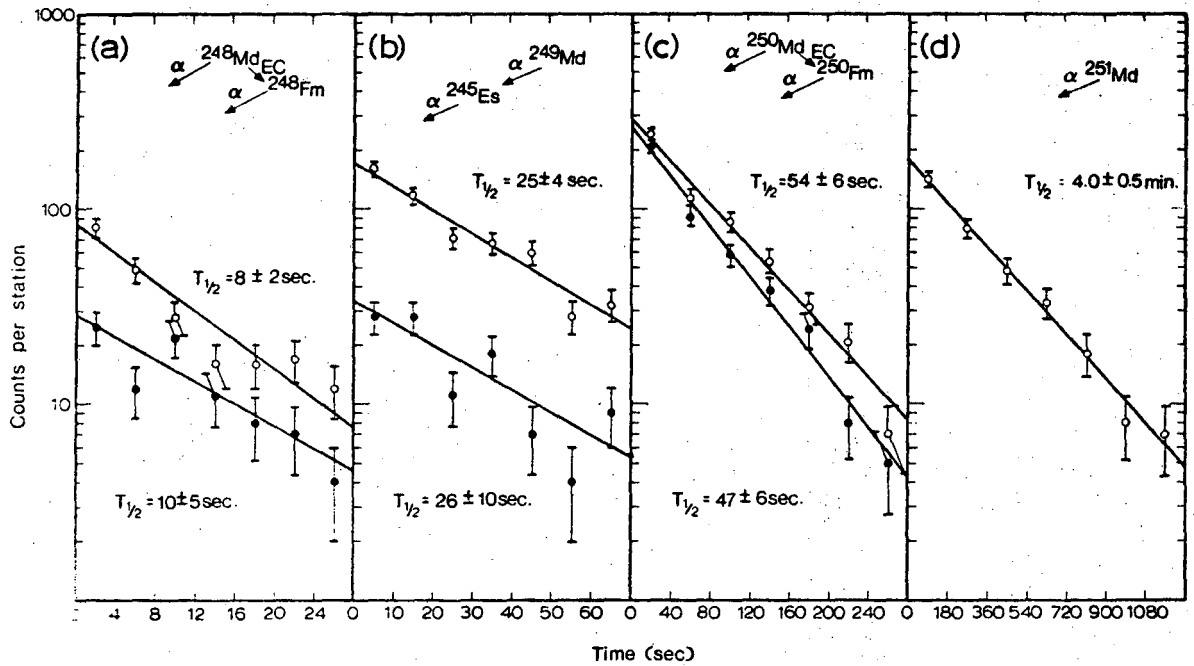
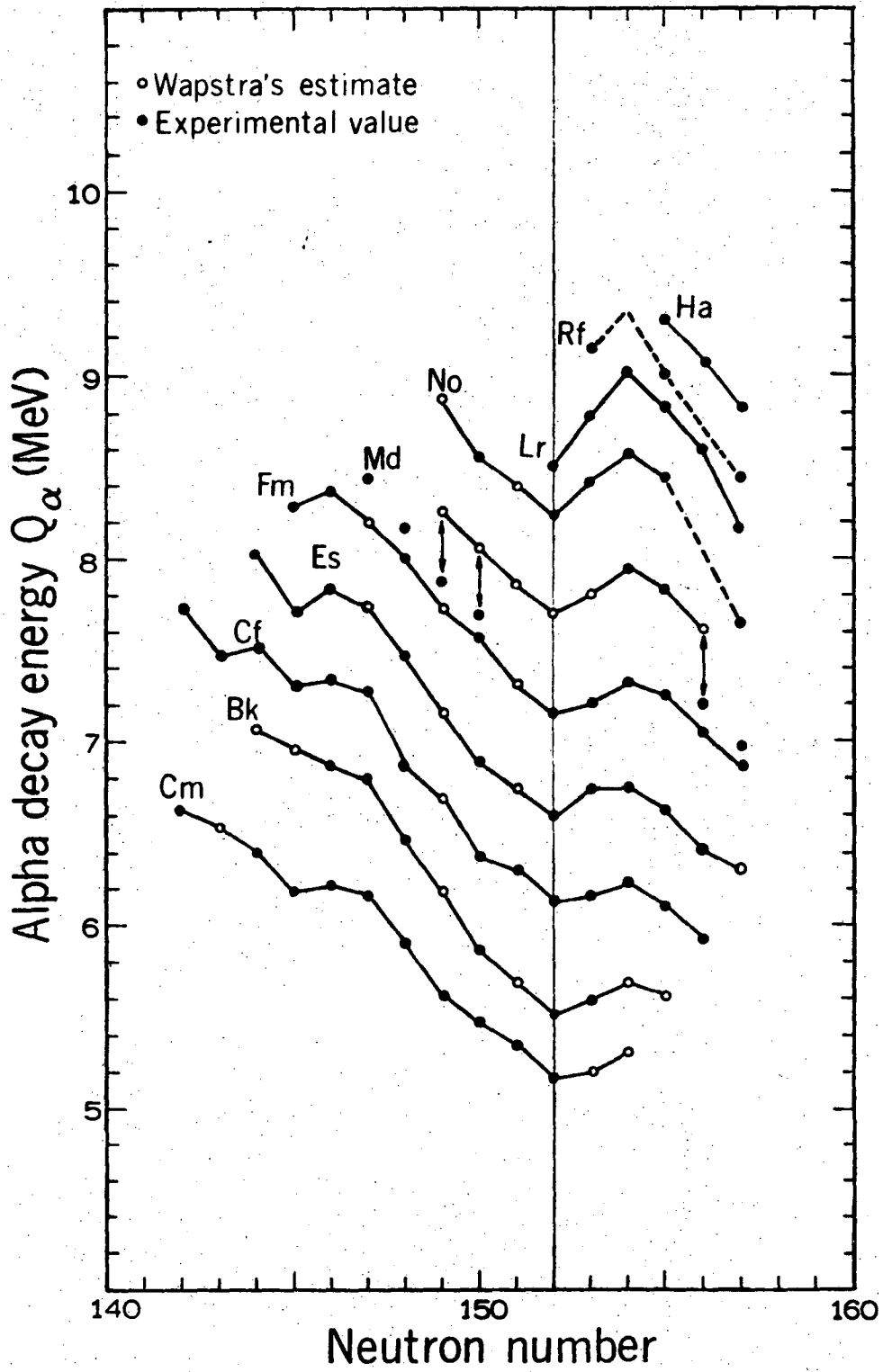


Fig. 8



XBL 723 5611

Fig. 9



XBL 7012 6271

Fig. 10

LEGAL NOTICE

*This report was prepared as an account of work sponsored by the United States Government. Neither the United States nor the United States Atomic Energy Commission, nor any of their employees, nor any of their contractors, subcontractors, or their employees, makes any warranty, express or implied, or assumes any legal liability or responsibility for the accuracy, completeness or usefulness of any information, apparatus, product or process disclosed, or represents that its use would not infringe privately owned rights.*

TECHNICAL INFORMATION DIVISION  
LAWRENCE BERKELEY LABORATORY  
UNIVERSITY OF CALIFORNIA  
BERKELEY, CALIFORNIA 94720